Pflugers Arch - Eur J Physiol
DOI 10.1007/s00424-016-1923-5

Increased bone resorption by osteoclast-specific deletion of the sodium/calcium exchanger isoform 1 (NCX1)

Giuseppe Albano[1,2,3,4,6] · **Silvia Dolder**[3,4] · **Mark Siegrist**[3,4] · **Annie Mercier-Zuber**[5,6] · **Muriel Auberson**[5,6] · **Candice Stoudmann**[5,6] · **Willy Hofstetter**[3,4] · **Olivier Bonny**[5,6] · **Daniel G. Fuster**[1,2,3,4,6]

Received: 26 August 2016 / Revised: 22 November 2016 / Accepted: 29 November 2016

Abstract Calcium is a key component of the bone mineral hydroxyapatite. During osteoclast-mediated bone resorption, hydroxyapatite is dissolved and significant quantities of calcium are released. Several calcium transport systems have previously been identified in osteoclasts, including members of the sodium/calcium exchanger (NCX) family. Expression pattern and physiological role of NCX isoforms in osteoclasts, however, remain largely unknown at the moment. Our data indicate that all three NCX isoforms (NCX1, NCX2, and NCX3) are present in murine osteoclasts. RANKL-induced differentiation of murine osteoclast precursors into mature osteoclasts significantly attenuated the expression of NCX1, while NCX2 and NCX3 expressions were largely unaffected. To study the role of NCX1 during osteoclast differentiation and bone resorption, we crossed mice with exon 11 of the *NCX1* gene flanked by loxP sites with cathepsin K-Cre transgenic mice. Mature osteoclasts derived from transgenic mice exhibited an 80–90% reduction of NCX1 protein. In vitro studies indicate that NCX1 is dispensable for osteoclast differentiation, but NCX1-deficient osteoclasts exhibited increased resorptive activity. In line with these in vitro findings, mice with an osteoclast-targeted deletion of the *NCX1* gene locus displayed an age-dependent loss of bone mass. Thus, in summary, our data reveal NCX1 as a regulator of osteoclast-mediated bone resorption.

Keywords Sodium/calcium exchanger · Bone · Osteoclast · NCX1

Olivier Bonny and Daniel G. Fuster contributed equally.

Electronic supplementary material The online version of this article (doi:10.1007/s00424-016-1923-5) contains supplementary material, which is available to authorized users.

✉ Daniel G. Fuster
Daniel.Fuster@ibmm.unibe.ch

[1] Division of Nephrology, Hypertension and Clinical Pharmacology, Bern University Hospital, University of Bern, Freiburgstrasse 15, 3010 Bern, Switzerland

[2] Institute of Biochemistry and Molecular Medicine, University of Bern, Bern, Switzerland

[3] NCCR Transcure, University of Bern, Bern, Switzerland

[4] Department of Clinical Research, University of Bern, Bern, Switzerland

[5] Department of Pharmacology and Toxicology, University of Lausanne, Lausanne, Switzerland

[6] NCCR Kidney.CH, University of Zürich, Zürich, Switzerland

Introduction

Tight control of the intracellular calcium concentration is critical for proper osteoclast differentiation [17]. During receptor activator of NF-κB ligand (RANKL)-induced osteoclast differentiation, cytosolic calcium concentrations display an oscillatory pattern directly influencing the calcineurin-dependent activation of the nuclear factor of activated T cell c1 (NFATc1), the key transcriptional activator of osteoclastogenic genes [20]. Once differentiated, osteoclasts are exposed to high ambient levels of calcium during the bone resorption process. Calcium concentrations in the resorptive hemivacuole can reach up to 40 mM, and calcium released into the hemivacuole during resorption is continuously transported out of the resorptive site [3, 19]. In situ studies on resorbing osteoclasts revealed that a large fraction of calcium released into the resorptive hemivacuole enters the cell and is subsequently released at the basolateral surface, indicating an important role of the transcellular calcium transport pathway in the osteoclast [3]. Transcellular transport of calcium in the osteoclast can theoretically occur via

Published online: 09 December 2016

transcytosis, as previously shown for organic and inorganic bone degradation products [16, 18] or via selective calcium channels and transporters present at the plasma membrane. The individual contributions of these two transport pathways with regard to transcellular transport of calcium in the osteoclast are currently unclear, but the following observations favor selective transcellular transport over transcytosis: (i) unlike matrix protein transcytosis that occurs after hours, calcium efflux at the basolateral surface commences within minutes upon seeding of osteoclasts on bone and occurs at constant rates [4]; (ii) transcytosis would involve cytosolic vacuoles with very high calcium concentrations which have not been reported to date.

A wide variety of plasmalemmal calcium transporters and channels have been described in osteoclasts, both at the apical and basolateral membranes, including ATP-driven plasma membrane calcium-ATPase (PMCA) isoforms 1 and 4 [11], transient receptor potential cation channel subfamily V member 5 (TRPV5) [22], the type 2 ryanodine receptor [14], stretch- and voltage-activated calcium channels [21, 23], and members of the sodium/calcium exchanger (NCX) family [12, 13]. The latter are bidirectional transporters that mediate the exchange of three sodium ions for a calcium ion, depending on the electrochemical gradient. Three different NCX isoforms exist (NCX1, NCX2, and NCX3). Of these, NCX1 and NCX3 exhibit several tissue-specific splice variants differing in a small region of the large intracellular loop [10]. While the expression of NCX isoforms during osteoclast differentiation remains unknown, mature osteoclasts were previously reported to express NCX1 and NCX3 but not NCX2 [12, 13]. NCX inhibitors or small interfering RNA (siRNA)-mediated knockdown of NCX1 or NCX3 suppressed osteoclastic pit resorption in vitro, indicating a critical role of NCX1 in osteoclast-mediated bone resorption [12, 13]. The goal of this study was to examine the expression patterns of

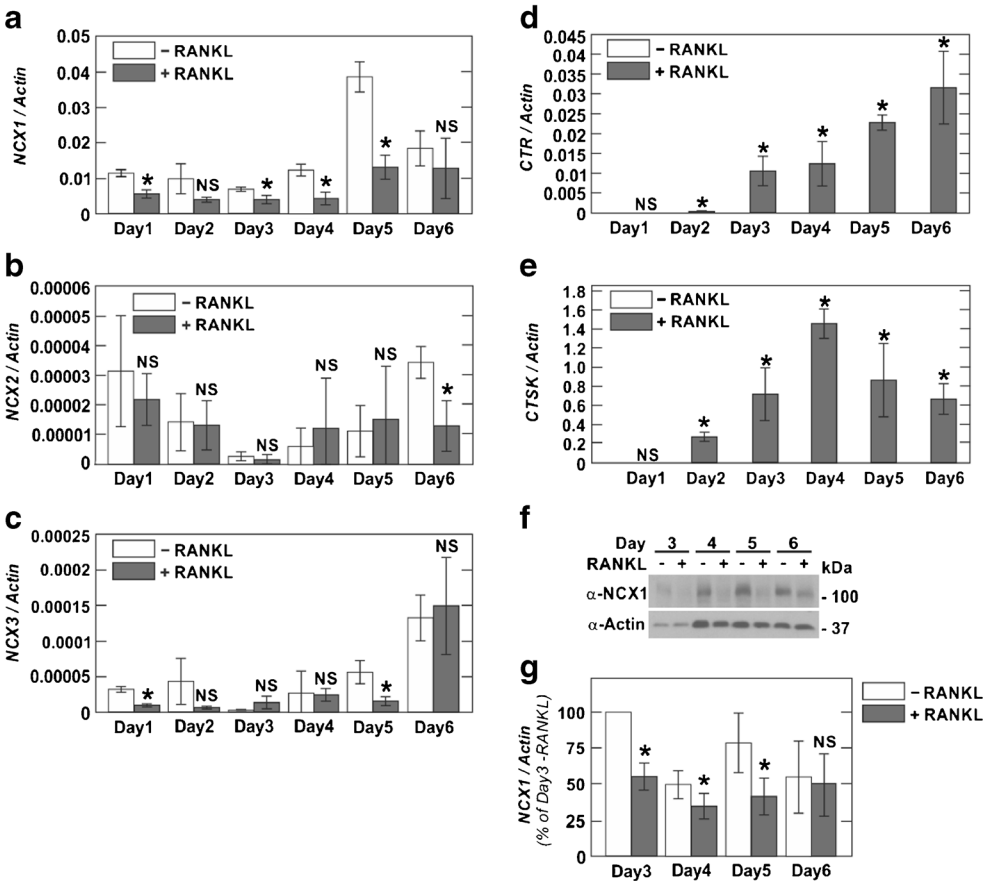

Fig. 1 Expression of NCX isoforms during osteoclast differentiation of bone marrow-derived monocytes. Primary M-CSF-dependent non-adherent osteoclast progenitor cells (OPCs) were cultured with or without RANKL for 6 days. **a**–**c** NCX1–3 transcript expression was assessed by real-time PCR analysis using Taqman probes. **d**, **e** Calcitonin receptor (CTR) and cathepsin K (CTSK) were used as markers of osteoclast differentiation. The amount of mRNA relative to β-actin was calculated using the ΔCt method. Values are shown as means ± SD; n = 3/group. $^*p < 0.05$; *NS*, not significant compared to vehicle treatment of same day. **f** NCX1 protein expression during osteoclast differentiation. At day 3 to day 6 of differentiation, cell lysates were prepared and equal amounts of protein (50 μg) were separated by SDS-PAGE and probed with indicated antibodies. **g** Quantification of immunoblotting. NCX1 protein expression relative to β-actin, normalized to day 3 vehicle treatment. Values are shown as means ± SD; n = 4/group. $^*p < 0.05$; *NS*, not significant compared to vehicle treatment of same day

NCX isoforms during osteoclast differentiation and to generate mice with osteoclast-specific deletion of NCX1 to study its role in bone homeostasis.

Results

Expression of NCX isoforms during osteoclast differentiation

We first analyzed expression of NCX isoforms during osteoclast differentiation using two different cell models, primary macrophage colony-stimulating factor (M-CSF)-dependent non-adherent osteoclast progenitor cells (OPCs) and cultured RAW 264.7 cells (Figs. 1 and 2). OPCs were cultured in the presence of 20 ng/ml RANKL and 30 ng/ml CSF-1 or in the presence of vehicle (0.1% BSA) and 30 ng/ml CSF-1 for a total of 6 days. RAW 264.7 cells were cultured in the presence of 50 ng/ml RANKL or in the presence of vehicle (0.1% BSA) for a total of 6 days. As shown in Figs. 1d, e and 2d, e, the transcript of the osteoclast differentiation markers calcitonin receptor (CTR) and cathepsin K (CTSK) were upregulated in a RANKL-dependent manner starting at day 2. In both OPCs and RAW 264.7 cells, all three NCX isoforms were expressed. Compared to vehicle-treated cells, RANKL stimulation attenuated NCX1 mRNA expression in both OPCs and RAW264.7 cells, but the effect was more pronounced in OPCs (Figs. 1a and 2a). Late during osteoclast differentiation at day 6, NCX1 transcript levels were again similar in both treatment groups in both OPCs and RAW264.7 cells. In support of these transcript expression results, NCX1 protein expression, normalized to β-actin, was lower in RANKL-treated than in vehicle-treated OPCs at days 3–5 of differentiation (Figs. 1f, g). In RAW264.7 cells, we observed a RANKL-dependent downregulation of NCX1 protein as well as of β-actin (Fig. 2f). NCX1 protein expression normalized to β-actin was similar in vehicle or RANKL-treated RAW264.7 cells throughout differentiation in RAW264.7 cells (Fig. 2g). The effect of

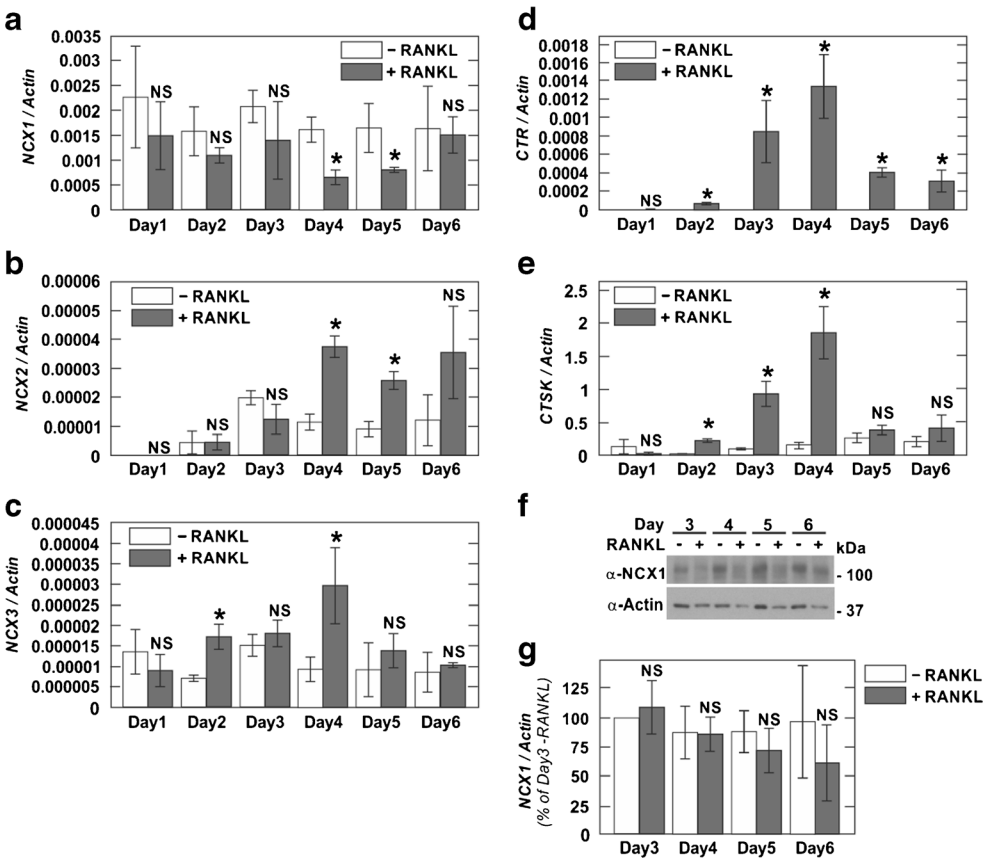

Fig. 2 Expression of NCX isoforms during osteoclast differentiation of RAW 264.7 cells. RAW 264.7 cells were cultured with or without RANKL for 6 days. **a**–**c** NCX1–3 transcript expression was assessed by real-time PCR analysis using Taqman probes. **d**, **e** Calcitonin receptor (CTR) and cathepsin K (CTSK) were used as markers of osteoclast differentiation. The amount of mRNA relative to β-actin was calculated using the ΔCt method. Values are shown as means ± SD; $n = 3$/group. *$p < 0.05$; *NS*, not significant compared to vehicle treatment. **f** NCX1 protein expression during osteoclast differentiation. At day 3 to day 6 of differentiation, cell lysates were prepared and equal amounts of protein (50 μg) were separated by SDS-PAGE and probed with indicated antibodies. **g** Quantification of immunoblotting. NCX1 protein expression relative to β-actin, normalized to day 3 vehicle treatment. Values are shown as means ± SD; $n = 4$/group. *$p < 0.05$; *NS*, not significant compared to vehicle treatment of same day

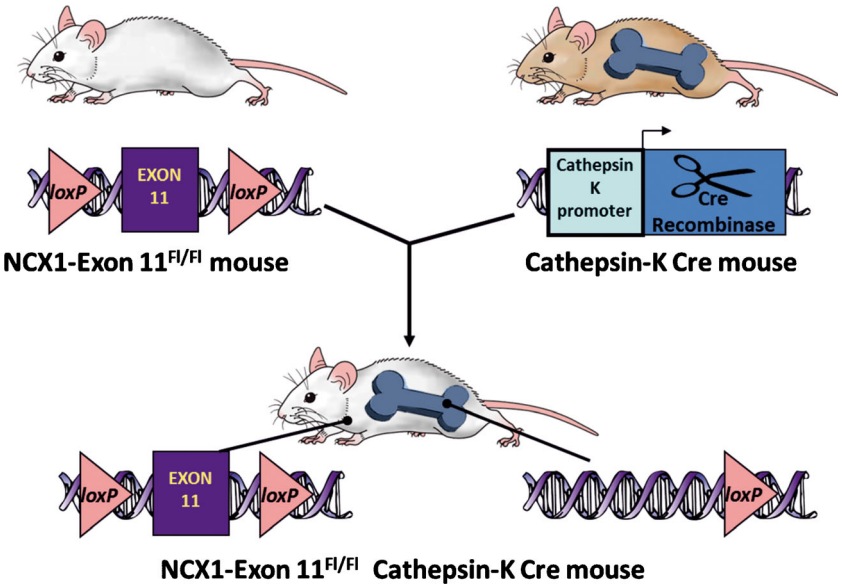

Fig. 3 Generation of osteoclast-specific NCX1-deficient ($NCX1^{\Delta OC/\Delta OC}$) mice. Mice with exon 11 of the *NCX1* gene flanked by loxP sites ($NCX1^{flox/flox}$) were crossed with *cathepsin-K Cre* ($Ctsk^{Cre/+}$) transgenic mice. Osteoclast-specific Cre recombinase activity results in osteoclast-specific NCX1-deficient mice ($Ctsk^{Cre/+}$; $NCX1^{flox/flox}$, herein named $NCX1^{\Delta OC/\Delta OC}$ mice)

RANKL treatment on NCX2 and NCX3 expression was minimal in OPCs (Fig. 1b, c). In RAW264.7 cells, RANKL treatment increased NCX2 expression beyond day 3 of differentiation (Fig. 2b). Starting at day 2 of differentiation, NCX3 was higher in RANKL-treated RAW264.7 cells, but the differences to vehicle-treated cells only reached statistical significance at days 2 and 4 of differentiation (Fig. 2c). Use of glyceraldehyde 3-phosphate dehydrogenase (GAPDH) as alternative housekeeping transcript for quantification of NCX transcript expression yielded results that were comparable to β-actin normalization (Suppl. Figs. 1 and 2).

Generation of osteoclast-specific NCX1-deficient mice

In a next step, we generated mice with osteoclast-specific deletion of the *NCX1* gene locus. To this end, we crossed mice with exon 11 of the *NCX1* gene flanked by loxP sites ($NCX1^{flox/flox}$) with *cathepsin-K Cre* ($Ctsk^{Cre/+}$) transgenic mice that express Cre recombinase under the promotor of the *CTSK* gene (Fig. 3) [7, 15]. Resulting osteoclast-specific NCX1-deficient mice ($Ctsk^{Cre/+}$; $NCX1^{flox/flox}$, herein named $NCX1^{\Delta OC/\Delta OC}$ mice) were born at expected Mendelian ratios without obvious phenotype. NCX1 protein levels in extraskeletal tissues (kidney and heart) of $NCX1^{\Delta OC/\Delta OC}$ were not different from $Ctsk^{Cre/+}$; $NCX1^{+/+}$ (herein named $NCX1^{+/+}$) mice (Fig. 4a–c). Weight of $NCX1^{\Delta OC/\Delta OC}$ mice was unaltered, and $NCX1^{\Delta OC/\Delta OC}$ mice displayed no abnormalities in renal electrolyte handling (Fig. 4d, e). Compared to $NCX1^{+/+}$ OPCs, $NCX1^{\Delta OC/\Delta OC}$ OPCs displayed NCX1 transcript reductions of ~70% at day 4 and of ~90% at day 5 during RANKL induction (Fig. 5a). The NCX1 transcript reduction was RANKL-dependent, with M-CSF treatment

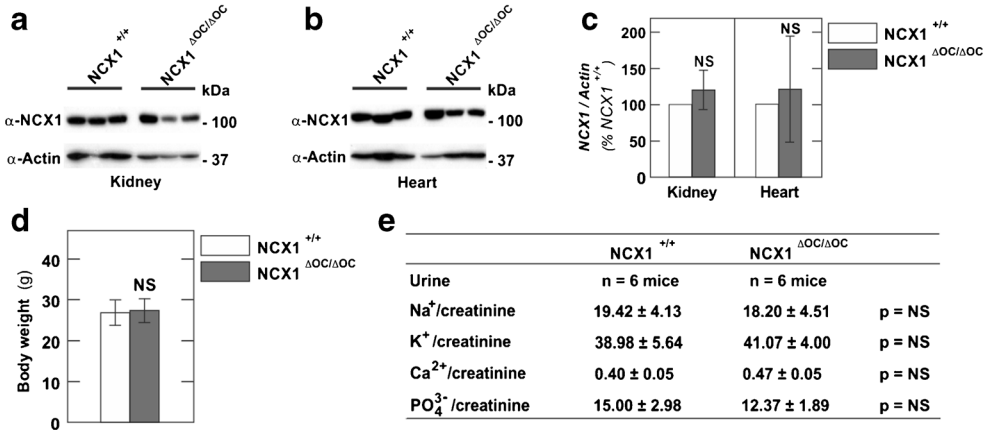

Fig. 4 Characterization of $NCX1^{\Delta OC/\Delta OC}$ mice. **a**, **b** NCX1 expression assessed by immunoblotting in extraosseous tissues of $NCX1^{\Delta OC/\Delta OC}$ mice and mice without NCX1 deletion ($Ctsk^{Cre/+}$; $NCX1^{+/+}$, herein named $NCX1^{+/+}$). **c** Quantification of NCX1 expression relative to actin in kidney and heart of $NCX1^{\Delta OC/\Delta OC}$ and $NCX1^{+/+}$ mice. Values are shown as means ± SD; *n* = 3/group. *NS* not significant. **d** Body weight of $NCX1^{\Delta OC/\Delta OC}$ and $NCX1^{+/+}$ mice at 3 months of age. **e** Urinary electrolytes of $NCX1^{\Delta OC/\Delta OC}$ and $NCX1^{+/+}$ mice at 3 months of age

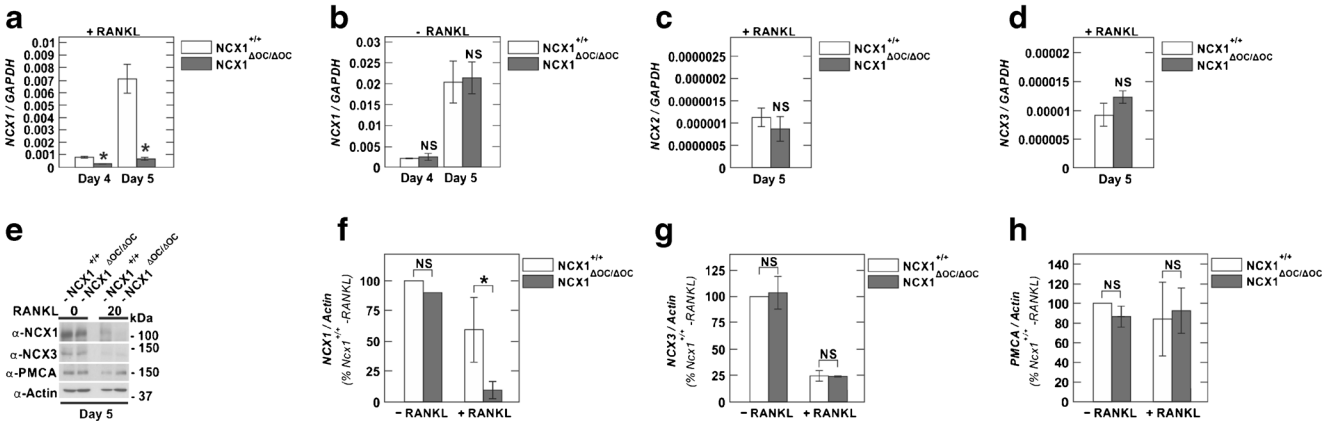

Fig. 5 Expression of NCX isoforms in NCX1$^{\Delta OC/\Delta OC}$ osteoclasts. Primary M-CSF-dependent non-adherent osteoclast progenitor cells (OPCs) of NCX1$^{\Delta OC/\Delta OC}$ and NCX1$^{+/+}$ mice were cultured with or without RANKL and harvested at indicated time points for RNA or protein isolation. **a** NCX1 transcript expression in the presence of RANKL at days 4 and 5. **b** NCX1 transcript expression in the absence of RANKL at days 4 and 5. **c** NCX2 transcript expression in the presence of RANKL at day 5. **d** NCX3 transcript expression in the presence of RANKL at day 5. NCX transcripts were quantified by real-time PCR using Taqman probes. The amount of NCX mRNA relative to GAPDH was calculated using the ΔCt method, $n = 3$ mice/group. *$p < 0.05$; *NS* not significant. **e** NCX1, NCX3, and PMCA protein expression in OPCs of NCX1$^{\Delta OC/\Delta OC}$ and NCX1$^{+/+}$ mice treated with or without RANKL at day 5. Equal amounts of protein (50 μg) were separated by SDS-PAGE and probed with indicated antibodies. **f** NCX1 protein expression in OPCs of NCX1$^{\Delta OC/\Delta OC}$ mice at day 5 of differentiation relative to β-actin, normalized to OPCs derived of NCX1$^{+/+}$ mice without RANKL, $n = 3$/group. *$p < 0.05$; *NS*, not significant compared to NCX1$^{+/+}$. **g** NCX3 protein expression in OPCs of NCX1$^{\Delta OC/\Delta OC}$ mice at day 5 of differentiation relative to β-actin, normalized to OPCs derived of NCX1$^{+/+}$ mice without RANKL, $n = 3$/group. *NS*, not significant compared to NCX1$^{+/+}$. **h** PMCA protein expression in OPCs of NCX1$^{\Delta OC/\Delta OC}$ mice at day 5 of differentiation relative to β-actin, normalized to OPCs derived of NCX1$^{+/+}$ mice without RANKL, $n = 3$/group. *$p < 0.05$; *NS* not significant. Values are shown as means ± SD

alone; NCX1 transcript levels were unaltered in NCX1$^{\Delta OC/\Delta OC}$ OPCs (Fig. 5b). Expression of the two other NCX isoforms NCX2 and NCX3, respectively, was similar in NCX1$^{+/+}$ and NCX1$^{\Delta OC/\Delta OC}$ OPCs (Fig. 5c, d). On protein level, NCX1 expression was reduced by 80–90% at day 5 of RANKL induction, whereas in the absence of RANKL treatment, no difference was observed between OPCs isolated from NCX1$^{+/+}$ and NCX1$^{\Delta OC/\Delta OC}$ mice (Fig. 5e, f). NCX3 protein expression was not altered in NCX1$^{\Delta OC/\Delta OC}$ OPCs (Fig. 5e, g). We also analyzed the expression of an alternative calcium exit pathway in the osteoclast, the PMCA. As shown in Fig. 5e, h, there were no differences in PMCA expression between OPCs isolated from NCX1$^{+/+}$ and NCX1$^{\Delta OC/\Delta OC}$ mice.

Differentiation and resorptive activity of NCX1$^{\Delta OC/\Delta OC}$ osteoclasts

We next assessed differentiation and resorptive activity of osteoclasts with NCX1 deficiency in vitro. For this purpose, OPCs from NCX1$^{+/+}$ and NCX1$^{\Delta OC/\Delta OC}$ mice were grown with or without 20 ng/ml RANKL and 30 ng/ml M-CSF. At days 4, 5, and 6 of the culture, cells were harvested and TRAP activity of cell lysates and the number of tartrate-resistant acid phosphatase positive (TRAP^{+}), multinucleated cells (MNC; ≥3 nuclei/cell) were quantified. As shown in Fig. 6a–d, differentiation into mature osteoclasts was not different in the cultures isolated from NCX1$^{\Delta OC/\Delta OC}$ mice compared to NCX1$^{+/+}$ mice. The resorptive activity of mature osteoclasts was determined according to [1, 24]. Osteoclasts were collected at day 5 of differentiation and seeded into calcium phosphate (CaP)-coated wells, containing ^{45}Ca as a tracer. Resorptive activity was calculated as ^{45}Ca released into the cell culture supernatant, normalized to TRAP activity 24 h after seeding. As shown in Fig. 6e, resorptive activity of NCX1$^{\Delta OC/\Delta OC}$ osteoclasts was significantly elevated compared to NCX1$^{+/+}$ osteoclasts.

Structural bone parameters of NCX1 $^{\Delta OC/\Delta OC}$ mice

To determine the impact of the enhanced resorptive activity of NCX1$^{\Delta OC/\Delta OC}$ osteoclasts observed in vitro on structural bone parameters, we performed high-resolution microcomputed tomography (μCT) studies on lumbar vertebrae of 3-month-old NCX1$^{+/+}$ and NCX1$^{\Delta OC/\Delta OC}$ mice. As depicted in Fig. 7a–e, we did not detect differences in bone volume or structural bone parameters between NCX1$^{+/+}$ and NCX1$^{\Delta OC/\Delta OC}$ mice at this age. However, at 6 months of age, μCT studies revealed a significantly reduced bone mass at all three lumbar sites in NCX1$^{\Delta OC/\Delta OC}$ mice (Fig. 7f–j). Connective density, trabecular number, and trabecular thickness showed all a trend for reduction in NCX1$^{\Delta OC/\Delta OC}$ mice, but the differences to NCX1$^{+/+}$ mice did not reach statistical significance. In contrast, trabecular space was higher in NCX1$^{\Delta OC/\Delta OC}$ mice; the differences reached statistical significance at the L5 site but not at the L3 and L4 sites.

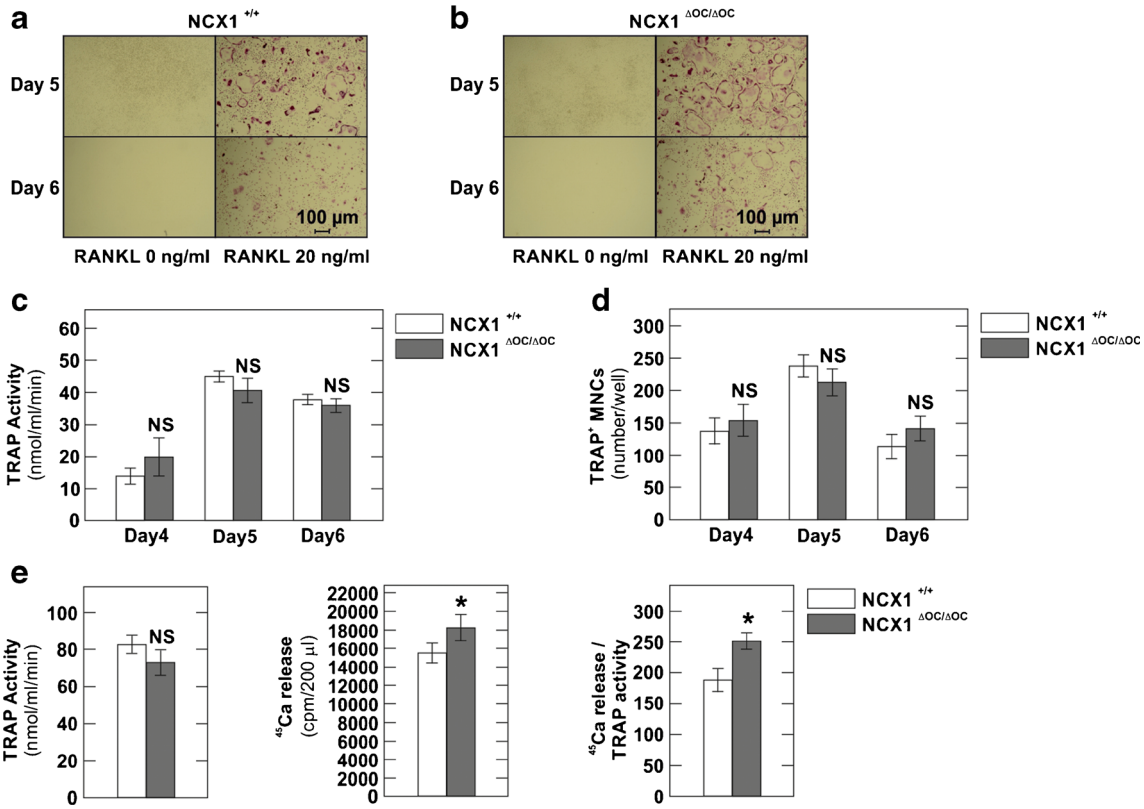

Fig. 6 In vitro characterization of $NCX1^{\Delta OC/\Delta OC}$ osteoclast differentiation and function. Primary M-CSF-dependent non-adherent osteoclast progenitor cells (OPCs) isolated from $NCX1^{\Delta OC/\Delta OC}$ and $NCX1^{+/+}$ mice were cultured with or without RANKL stimulation for the indicated time. **a** Representative TRAP staining images of $NCX1^{\Delta OC/\Delta OC}$ OPC cultures. **b** Representative TRAP staining images of $NCX1^{+/+}$ OPC cultures. **c** TRAP activity after 4, 5, or 6 days of stimulation, (n = 30/group/day, 5 mice/group). **d** Quantification of $TRAP^+$ multinucleated cells (MNC; ≥3 nuclei/cell) after 4, 5, or 6 days of stimulation, (n = 30/group/day, 5 mice/group). **e** Resorptive activity of osteoclasts. *Left panel*: TRAP activity of osteoclast cultures 24 h after reseeding on calcium-phosphate coated plates. *Middle panel*: ^{45}Ca release in the supernatant after 24 h. *Right panel*: resorptive activity of osteoclast cultures, quantified as ^{45}Ca released in the supernatant normalized to TRAP activity; n = 30/group, 5 mice/group. Data are shown as mean ± SD. *$p < 0.05$; *NS* not significant

Discussion

Our expression analysis revealed that all three NCX isoforms are expressed in osteoclast progenitors and mature osteoclasts. We find that NCX1 but not NCX2 or NCX3 is downregulated during RANKL-induced osteoclast differentiation of primary OPCs. In analogy with a previous study employing the NCX inhibitors SEA0400 and KB-R7943, genetically induced NCX1 deficiency did not affect differentiation of primary OPCs into mature osteoclasts [12]. An important difference to previous studies with NCX inhibitors, however, is the timing of NCX deficiency in our model. NCX1 deletion in osteoclasts occurs in parallel to cathepsin K expression. The latter starts at day 2 of RANKL stimulation but reaches maximal levels only at day 4. Thus, maximal deletion efficiency occurs late during osteoclast differentiation and mainly affects mature osteoclasts. We can, therefore, not completely rule out the possibility that NCX1 plays a critical role in osteoclast differentiation.

However, and in contradiction to previous studies employing pharmacological NCX inhibition or siRNA-mediated knockdown of NCX1 in osteoclasts, our experiments revealed increased resorptive activity of genetically induced NCX1-deficient osteoclasts. The reason for this discrepancy is not clear, but several aspects warrant special consideration: inhibition of resorption by the NCX inhibitors SEA0400 and KB-R7943 was only observed at very high concentrations (10–100 μM), well above the individual IC_{50} values of the inhibitors. At such concentrations, off-target effects have been reported for these NCX inhibitors, including inhibition of voltage-sensitive sodium channels, L-type calcium channels, inward rectifying potassium channels, and attenuation of store-operated calcium entry [2]. In support of the latter, SEA0400, a highly potent NCX1 inhibitor (IC_{50} 0.01–0.1 μM), did not affect resorption in concentrations up to 5 μM. SEA0400 was even less effective in resorption inhibition than the less potent NCX1 inhibitor KB-R7943 (IC_{50} 0.5–5 μM) [2, 9]. Furthermore, it is well known that SEA0400 and KB-R7943 inhibit NCX reverse mode only (cellular sodium extrusion and calcium uptake) with little effect on forward mode transport [9]. In contrast, the genetic deletion used in our study will affect all modes of NCX1 transport. Assuming that both modes of NCX1 transport occur during the bone resorption process

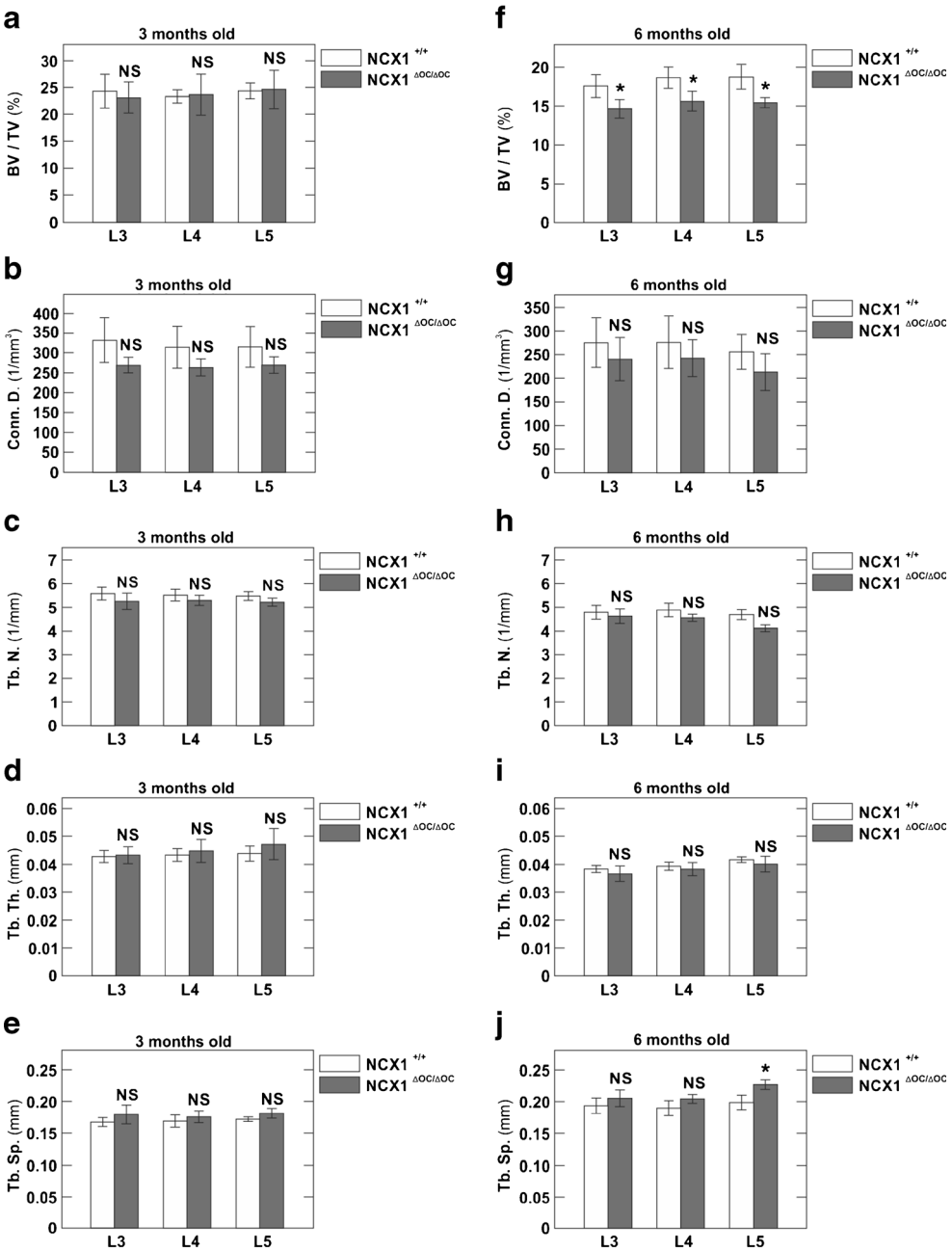

Fig. 7 Structural bone parameters of NCX1$^{\Delta OC/\Delta OC}$ mice. Lumbar vertebrae (nos. 3, 4, and 5) at 3 or 6 months of age were isolated and analyzed by μCT. **a**–**e** Histograms representing structural parameters of lumbar vertebrae of 3-month-old mice. **f**–**j** Histograms representing structural parameters of lumbar vertebrae of 6-month-old mice. Bone volume/total volume fraction (*BV/TV*), connective density (*Conn.D.*), trabecular number (*Tb.N.*), trabecular thickness (*Tb.Th.*), trabecular space (*Tb.Sp.*). Data are shown as mean ± SD, $n = 5$ mice/group. *$p < 0.05$; *NS* not significant

(either sequentially or in parallel due to expression of NCX1 at different surface membranes of the osteoclast), it is conceivable that selective reverse mode inhibition indeed selectively inhibits bone resorption. Thus, regardless of the potential mechanism involved (off-target effect or selective reverse mode inhibition), the potential of NCX inhibitors in preventing bone loss should be further explored in future studies.

One previous study reported inhibition of resorption by selective siRNA-mediated knockdown of the NCX1A or 1B isoform in mature osteoclasts [12]. These data stand in contradiction to our results revealing increased resorptive activity upon genetic deletion of NCX1 in osteoclasts. Knockdown efficiencies in that peculiar study were low; however, NCX1A and 1B transcripts were reduced by 29 and 34%, respectively, compared to control [12]. In contrast, all NCX1 transcripts are affected by Cre-mediated deletion of exon 11 of the *NCX1* gene in our transgenic model and the reduction of NCX1 mRNA and protein is far more pronounced. Furthermore, Cre-mediated deletion already starts at day 2 of RANKL treatment, whereas siRNA-mediated knockdown was performed in mature osteoclast. Thus, time point and degree of NCX1 reduction or the type of NCX1 isoform(s) targeted may be the cause for the differences observed between the two studies.

Regardless of the discrepancies to previous in vitro studies, however, our μCT studies indicate that there is an age-dependent loss of bone mass in transgenic NCX1$^{\Delta OC/\Delta OC}$ mice.

Our in vivo results in mice are supported by our in vitro findings demonstrating increased resorptive activity of NCX1-deficient osteoclasts. Limitations of our study are the absence of histomorphometry data and the fact that we did not perform measurements of bone resorption markers in blood and urine.

In summary, our data suggest that NCX1 physiologically attenuates bone resorption in osteoclasts and argue against an osteoprotective effect of non-selective NCX1 inhibition.

Materials and methods

Unless specified otherwise, all chemicals and reagents were obtained from Sigma. Statistical analysis was done using Student's *t* test. All statistical tests were two-sided, and a p value <0.05 was considered statistically significant.

Cell culture and osteoclast differentiation

The murine macrophage/monocyte cell line RAW 264.7 was obtained from ATCC. Cells were maintained in α-MEM (Invitrogen, Carlsbad, CA), supplemented with 10% FBS (Invitrogen), 100 U/ml penicillin and 100 U/ml streptomycin, and grown in a humidified 95/5% air/CO_2 atmosphere incubator at 37 °C. To induce osteoclast differentiation, RAW 264.7 cells were cultured in the presence of 50 ng/ml soluble RANKL (PeproTech, Hamburg, Germany) for indicated time points with changes of medium and RANKL every other day. Primary osteoclasts were prepared from M-CSF-dependent non-adherent osteoclast progenitor cells (OPCs) as described [1, 8]. Femora and tibiae of 8- to 10-week-old mice were dissected and bone marrow cells flushed out with Hanks' balanced salt solution supplemented with 100 U/ml penicillin and 100 U/ml streptomycin. Cells were then sedimented, resuspended, counted, and plated in α-MEM supplemented with 10% FBS in the presence of 30 ng/ml M-CSF (Chiron, Emeryville, CA) and 20 ng/ml RANKL with medium changes every 2 days.

In vitro osteoclast resorption assay

To determine the capacity of osteoclasts to dissolve mineral, mature osteoclasts were seeded onto a layer of CaP. Similarly, as described before [24], solutions of 0.12 M Na_2HPO_4 and 0.2 M $CaCl_2$ in 50 mM Tris/HCl pH 7.4 were preincubated overnight in a 5% CO_2 incubator at 37 °C. Equal volumes were mixed and a CaP slurry precipitated. After washing twice with water, the slurry was resuspended in 1 ml of water/90 μl slurry. To the CaP suspension, $^{45}CaCl_2$ (PerkinElmer, Schwerzenbach, CH) was added to a specific activity of 1700 Bq/20 μg slurry. Of the spiked suspension, 200 μl was distributed into wells of 48-well plates, dried at room temperature for 3 days, and baked at 80 °C for 3 h. Before use, the CaP-coated plates were equilibrated with 30% FBS in cell culture medium over night. Osteoclasts were generated in cultures of OPC for 5 days with M-CSF (30 ng/ml) and RANKL (20 ng/ml) in 5-cm-diameter UpCell dishes (Thermo Fisher Scientific Inc., Waltham, MA, USA) as described above. Mature osteoclasts were detached from the dishes by incubating the plates at 4 °C. The cells from one UpCell dish were resuspended in 500 μl α-MEM/FBS/M-CSF/RANKL, and 50 μl was distributed into the CaP-coated 48-well plates. After 24 h, the cell supernatants were collected and the solubilized ^{45}Ca was counted in a scintillation counter.

Osteoclast-specific NCX1-deficient mice

All animal experiments were in accordance with the Swiss Animal Welfare Law and were approved by the Local Veterinary Authority Bern (Veterinäramt Bern) and Vaud (Office vétérinaire cantonal). Mice had free access to water and standard chow diet (no. 3436 from Provimi Kliba AG, Kaiseraugst, Switzerland) and were maintained on a 12 h light/12 h dark cycle. Generation and characterization of mice with exon 11 of NCX1 flanked by loxP sites ($NCX1^{flox/flox}$ mice) were described previously [7]. To obtain osteoclast-specific NCX1 deletion, $NCX1^{flox/flox}$ were bred with mice expressing Cre recombinase under the cathepsin K promoter ($Ctsk^{Cre/+}$mice) [15]. For all experiments, only male mice were used. All experiments were performed on mice backcrossed at least 10 generations into C56BL/6J background.

RNA isolation, RT-PCR, and quantitative real-time PCR

Total RNA was isolated using Trizol® reagent as detailed in the manufacturer's protocol (Invitrogen, Carlsbad, CA). Reverse transcription was performed using the Taqman® Reverse Transcription kit (Life Technologies/ABI, Rotkreuz, CH). PCR was performed as described previously [6]. Real-time PCR was performed using presynthesized Taqman®-based Assays-on-Demand (Life Technologies/ABI, Rotkreuz, CH) on an ABI ViiA 7 System. The following AoDs were employed: NCX1 (Mm00441524_m1), NCX2 (Mm0055836_m1), NCX3 (Mm00475520_m1), Calcitonin receptor (Mm00432282_m1), cathepsin K (Mm00484039_m1), GAPDH (Mm99999915_g1), and β-actin (Mm04394036_g1). The efficiencies of all primers were determined in our laboratory using a dilution series (5 logs) and were as follows: NCX1, 99.40%; NCX2, 99.22%; NCX3, 99.41%; GAPDH, 99.43%; and β-actin, 99.54%. Ct values for triplicate technical replicates were averaged, and the amount of mRNA relative to GAPDH or β-actin was calculated using the ΔCt method.

Antibodies and immunoblotting

Antibodies used in the study were from the following sources: monoclonal anti-α_1 subunit of Na/K-ATPase (Millipore,

Billerica, MA), polyclonal anti-β-actin (Santa Cruz Biotechnology, Santa Cruz, CA), monoclonal anti-NCX1 (Swant, Bellinzona, Switzerland), polyclonal anti-NCX3 (Cosmo Bio Ltd. Tokyo, Japan), and monoclonal pan anti-PMCA (Thermo Fisher Scientific, Rockford, IL). Immunoblotting was performed as described [6].

Micro-CT analysis

Bone structure was determined in a μCT40 System (Scanco, Brüttisellen, Switzerland). For this purpose, freshly excised bone specimen were fixed in 4% paraformaldehyde, rinsed overnight with tap water, and immersed in 70% ethanol. MicroCT scans were performed in 70% ethanol at the highest resolution, with a voxel size of 8 μm [5].

Acknowledgements We thank Kenneth Philippson, Department of Physiology, David Geffen School of Medicine, UCLA for NCX1 mutant mice. DGF was supported by the Swiss National Science Foundation (grant nos. 3100A0_135503 and 3100A0_152829) and by a Medical Research Position Award of the Foundation Prof. Dr. Max Cloëtta. OB is supported by a Swiss National Science Foundation professorship grant (PP00P3-133648). This work was further supported by the Swiss National Science Foundation funded National Centers for Competence in Research (NCCR Transcure and NCCR Kidney.CH) to DGF, OB, and WH.

Compliance with ethical standards All animal experiments were in accordance with the Swiss Animal Welfare Law and were approved by the Local Veterinary Authority Bern (Veterinäramt Bern) and Vaud (Office vétérinaire cantonal).

Conflict of interest The authors declare that they have no conflict of interest.

References

1. Albano G, Moor M, Dolder S, Siegrist M, Wagner CA, Biber J, Hernando N, Hofstetter W, Bonny O, Fuster DG (2015) Sodium-dependent phosphate transporters in osteoclast differentiation and function. PLoS One 10:e0125104
2. Amran MS, Homma N, Hashimoto K (2003) Pharmacology of KB-R7943: a Na+-Ca2+ exchange inhibitor. Cardiovasc Drug Rev 21: 255–276
3. Berger CE, Rathod H, Gillespie JI, Horrocks BR, Datta HK (2001) Scanning electrochemical microscopy at the surface of bone-resorbing osteoclasts: evidence for steady-state disposal and intracellular functional compartmentalization of calcium. J Bone Miner Res 16:2092–2102
4. Datta HK, Horrocks BR (2003) Mechanisms of calcium disposal from osteoclastic resorption hemivacuole. J Endocrinol 176:1–5
5. Egermann M, Heil P, Tami A, Ito K, Janicki P, Von Rechenberg B, Hofstetter W, Richards PJ (2009) Influence of defective bone marrow osteogenesis on fracture repair in an experimental model of senile osteoporosis. J Orthop Res.
6. Fuster DG, Zhang J, Shi M, Bobulescu IA, Andersson S, Moe OW (2008) Characterization of the sodium/hydrogen exchanger NHA2. J Am Soc Nephrol 19:1547–1556
7. Henderson SA, Goldhaber JI, So JM, Han T, Motter C, Ngo A, Chantawansri C, Ritter MR, Friedlander M, Nicoll DA, Frank JS, Jordan MC, Roos KP, Ross RS, Philipson KD (2004) Functional adult myocardium in the absence of Na+-Ca2+ exchange: cardiac-specific knockout of NCX1. Circ Res 95:604–611
8. Hofstetter W, Siegrist M, Simonin A, Bonny O, Fuster DG (2010) Sodium/hydrogen exchanger NHA2 in osteoclasts: subcellular localization and role in vitro and in vivo. Bone 47:331–340
9. Iwamoto T, Kita S, Uehara A, Imanaga I, Matsuda T, Baba A, Katsuragi T (2004) Molecular determinants of Na+/Ca2+ exchange (NCX1) inhibition by SEA0400. J Biol Chem 279:7544–7553
10. Khananshvili D (2014) Sodium-calcium exchangers (NCX): molecular hallmarks underlying the tissue-specific and systemic functions. Pflügers Archiv European Journal of Physiology 466:43–60
11. Kim HJ, Prasad V, Hyung SW, Lee ZH, Lee SW, Bhargava A, Pearce D, Lee Y, Kim HH (2012) Plasma membrane calcium ATPase regulates bone mass by fine-tuning osteoclast differentiation and survival. J Cell Biol 199:1145–1158
12. Li JP, Kajiya H, Okamoto F, Nakao A, Iwamoto T, Okabe K (2007) Three Na+/Ca2+ exchanger (NCX) variants are expressed in mouse osteoclasts and mediate calcium transport during bone resorption. Endocrinology 148:2116–2125
13. Moonga BS, Davidson R, Sun L, Adebanjo OA, Moser J, Abedin M, Zaidi N, Huang CL, Zaidi M (2001) Identification and characterization of a sodium/calcium exchanger, NCX-1, in osteoclasts and its role in bone resorption. Biochem Biophys Res Commun 283:770–775
14. Moonga BS, Li S, Iqbal J, Davidson R, Shankar VS, Bevis PJ, Inzerillo A, Abe E, Huang CL, Zaidi M (2002) Ca(2+) influx through the osteoclastic plasma membrane ryanodine receptor. Am J Physiol Renal Physiol 282:F921–F932
15. Nakamura T, Imai Y, Matsumoto T, Sato S, Takeuchi K, Igarashi K, Harada Y, Azuma Y, Krust A, Yamamoto Y, Nishina H, Takeda S, Takayanagi H, Metzger D, Kanno J, Takaoka K, Martin TJ, Chambon P, Kato S (2007) Estrogen prevents bone loss via estrogen receptor alpha and induction of Fas ligand in osteoclasts. Cell 130:811–823
16. Nesbitt SA, Horton MA (1997) Trafficking of matrix collagens through bone-resorbing osteoclasts. Science 276:266–269
17. Nowycky MC, Thomas AP (2002) Intracellular calcium signaling. J Cell Sci 115:3715–3716
18. Salo J, Lehenkari P, Mulari M, Metsikko K, Vaananen HK (1997) Removal of osteoclast bone resorption products by transcytosis. Science 276:270–273
19. Silver IA, Murrills RJ, Etherington DJ (1988) Microelectrode studies on the acid microenvironment beneath adherent macrophages and osteoclasts. Exp Cell Res 175:266–276
20. Takayanagi H, Kim S, Koga T, Nishina H, Isshiki M, Yoshida H, Saiura A, Isobe M, Yokochi T, Inoue J, Wagner EF, Mak TW, Kodama T, Taniguchi T (2002) Induction and activation of the transcription factor NFATc1 (NFAT2) integrate RANKL signaling in terminal differentiation of osteoclasts. Dev Cell 3:889–901
21. Teti A, Grano M, Colucci S, Argentino L, Barattolo R, Miyauchi A, Teitelbaum SL, Hruska KA, Zambonin Zallone A (1989) Voltage dependent calcium channel expression in isolated osteoclasts. Boll Soc Ital Biol Sper 65:1115–1118
22. van der Eerden BC, Hoenderop JG, de Vries TJ, Schoenmaker T, Buurman CJ, Uitterlinden AG, Pols HA, Bindels RJ, van Leeuwen JP (2005) The epithelial Ca2+ channel TRPV5 is essential for proper osteoclastic bone resorption. Proc Natl Acad Sci U S A 102:17507–17512
23. Wiltink A, Nijweide PJ, Scheenen WJ, Ypey DL, Van Duijn B (1995) Cell membrane stretch in osteoclasts triggers a self-reinforcing Ca2+ entry pathway. Pflugers Arch 429:663–671
24. Xie W, Lorenz S, Dolder S, Hofstetter W (2016) Extracellular iron is a modulator of the differentiation of osteoclast lineage cells. Calcif Tissue Int 98:275–283